Proc. Natl. Acad. Sci. USA
Vol. 90, pp. 6390–6394, July 1993
Biochemistry

Targeting the site of RNA–RNA recombination in brome mosaic virus with antisense sequences

(mechanism/heteroduplex formation)

PETER D. NAGY AND JOZEF J. BUJARSKI*

Plant Molecular Biology Center and Department of Biological Sciences, Northern Illinois University, DeKalb, IL 60115

Communicated by Paul Kaesberg, March 18, 1993

ABSTRACT **It has been postulated that local hybridizations between viral RNAs can mediate recombination in brome mosaic virus (BMV) and in poliovirus. To test this model, a 3′ fragment of BMV RNA1 was inserted into the 3′ noncoding sequence of BMV RNA3 in an antisense orientation. This resulted in high-frequency nonhomologous crossovers at or near the hybridized region. Insertion of the same RNA1 fragment in a positive-sense orientation did not promote recombination. Modification of the antisense insert by deletion of 3′ portions did not affect the sites of crossover. However, modification of the 5′ portion shifted the crossovers toward the central part of the heteroduplex region. Our results provide experimental evidence that recombinant crosses can be primed by hybridization between viral RNA molecules.**

Genetic recombination in RNA viruses provides a means to repair their genomes, to increase genetic variability, and to facilitate evolution (1, 2). We have studied genetic recombination in brome mosaic virus (BMV), a plant single-stranded RNA virus. The genome of BMV includes three RNA segments that share homologous sequences within their 3′ noncoding regions (3). RNA–RNA recombination in BMV was first demonstrated after coinoculation with a mixture of wild-type (wt) RNA1, wt RNA2, and a mutated RNA3 (designated M4). M4 contained a short deletion in the 3′ noncoding sequence (4). The repaired RNA3 progeny resulted from crossovers between M4 RNA3 and either RNA1 or RNA2. In a majority of recombinants, the crosses occurred at homologous (legitimate) positions, while some contained duplications of 3′ noncoding sequences. Characterization of a large number of recombinants suggested that BMV RNAs can form local heteroduplexes at the crossover sites (5, 6).

In addition to two bromoviruses, BMV and cowpea chlorotic mottle virus (CCMV) (7–10), RNA–RNA recombination has been demonstrated experimentally in other plant viruses (11, 12), in animal viruses (13–17), and in bacteriophages (18, 19). As in BMV, formation of local heteroduplexes was proposed to promote RNA–RNA recombination in poliovirus RNAs (14) or to be involved in generation of poliovirus defective interfering RNAs (15). Using poliovirus mutants to inhibit the replication of one parent, Kirkegaard and Baltimore (13) showed that recombination occurs via a copy-choice mechanism. In Sindbis virus, mutated RNAs induced illegitimate recombinants that contained both viral and nonviral insertions (17), most likely via a mechanism analogous to that observed in bromoviruses.

A discontinuous copy-choice mechanism has been proposed for recombination between genomic, defective interfering, and satellite RNAs of turnip crinkle virus (11, 20). The acceptor crossover sites appeared to correspond to the recognition sequences of the turnip crinkle virus RNA replicase. Some form of discontinuous recombination mechanism also has been postulated for mouse hepatitis coronavirus (16). The crossover hotspots resulted from selection rather than from specific sequences (21), suggesting a random nature of recombination for mouse hepatitis coronavirus.

In the present study, we provide experimental evidence for hybridization-mediated recombination in BMV. RNA3 constructs carrying antisense RNA1 sequences have been used to direct crossovers between RNA1 and RNA3 at or near the site of hybridization. We find that both the incidence of recombination and the location of recombinant junctions depend on the structure and stability of heteroduplex regions.

MATERIALS AND METHODS

Materials. Plasmids pB1TP3, pB2TP5, pB3TP7, and pCC3TP4 (a generous gift of Paul Ahlquist, University of Wisconsin, Madison)—containing full-length cDNA copies of wt BMV RNA components 1, 2, and 3 and CCMV RNA3, respectively—were used to synthesize infectious viral RNA transcripts (22, 23). The following primers were used in this study (the mutated sequences are underlined): 1, CAGTGAATTCTGGTCTCTTTTAGAGATTTACAG; 2, CTGAAGCAGTGCCTGCTAAGGCGGTC; 3, CAGTGAATTCTTTCGACTAGGCGCTGCCCACCA; 4, CAGTACTAGTTTAAGTGATGCGCTTGTCTC; 5, CAGTACTAGTCGCTTGTCTCTGTGTGAGACC; 6, CAGTACTAGTTGTGTGAGACCTCTGCTCGA; 7, TAGTCTCGAGCAGAGGTTTTATATAGAGACAAGCGCATCA; 8, CTAGTCTCGAGGTCTCACAGGATCCAGACAAGCGCATCACTTAACAC; 9, ACAGGATCCAGACAAGCGACGCGTACTTAACACGCTAGCTAAAGATCAAATCACCAG.

Plasmid Construction. The PN*x* plasmids (described below) are derivatives of pB3TP7, from which infectious BMV RNA3 can be synthesized *in vitro* (22). To construct PN0 (Fig. 1), PCR mutagenesis (24) with primers 2 and 3 was used to place a 197-bp fragment of pCC3TP4 (positions 1954–2150; ref. 23) into a pB3DM4 construct (6) between *Ban* II and *Hin*dIII restriction sites.

To generate PN1(−), a *Dra* I–*Xho* I fragment of pB1TP3 (positions 243–382, counted from the 3′ end) was blunt-end ligated into PN0 at the unique *Spe* I site (Fig. 1). The constructs PN2(−) and PN2(+) were obtained in the same way as PN1(−) except that the *Sac* I–*Xho* I fragment of pB1TP3 (positions 243–308) was inserted in antisense and sense orientations, respectively. PN2(−)NR was generated by digestion of PN2(−) with *Kpn* I and *Eco*RI (Fig. 1), treatment with T4 DNA polymerase, addition of *Eco*RI linkers, and religation of the desired fragment isolated by agarose electrophoresis.

The publication costs of this article were defrayed in part by page charge payment. This article must therefore be hereby marked "*advertisement*" in accordance with 18 U.S.C. §1734 solely to indicate this fact.

Abbreviations: BMV, brome mosaic virus; CCMV, cowpea chlorotic mottle virus; wt, wild type; RT-PCR, reverse transcription–polymerase chain reaction.

*To whom reprint requests should be addressed.

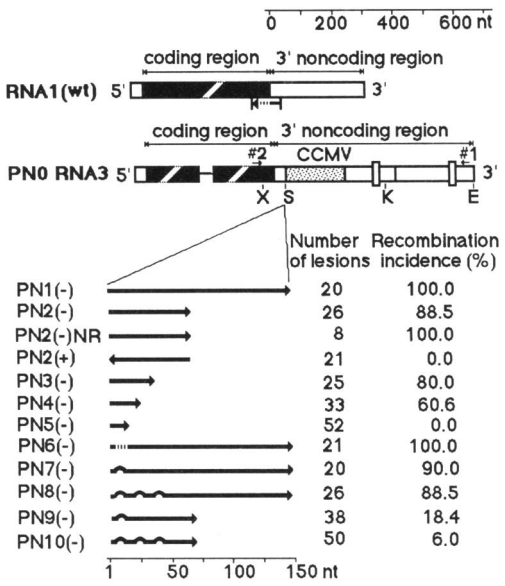

FIG. 1. (*Upper*) Schematic representation of the 3′ terminal noncoding regions in the wt BMV RNA1 and in mutated BMV RNA3 constructs. The RNA3 mutants [PN1(−) through PN10(−)] are all derivatives of PN0 RNA3, which has a mutated 3′ noncoding region with sequence duplication (described in ref. 6). In addition to the above duplication, the 3′ noncoding region of PN0 contains a 197-nt 3′ noncoding sequence of CCMV RNA3 (stippled box). The location of primers used for reverse transcription–polymerase chain reaction (RT–PCR) analysis (see Fig. 2) is shown by short horizontal arrows above the PN0 construct. X, S, K, and E mark the positions of *Xba* I, *Spe* I, *Kpn* I, and *Eco*RI restriction sites, respectively. For estimation of the total length of the 3′ noncoding region, see scale at the top. Coding regions, an intercistronic RNA3 region, and 5′ noncoding regions (not to scale) are represented by solid boxes, a short horizontal line, and open boxes, respectively. The location of RNA1 sequences used as inserts is marked by a horizontal arrow below the RNA1 molecule (the head of the arrow shows the sense orientation). (*Lower*) PN1(−) through PN10(−) were obtained by ligation of RNA1-specific cDNA sequences (represented by solid horizontal arrows) into PN0 at the *Spe* I site. The sense or antisense orientations of the inserts are shown by the heads of the arrows. The dotted region on the left side of the PN6(−) arrow depicts the area of C → U mutations, and one or three small curves in PN7(−) to PN10(−) arrows represent mismatch mutations. PN2(−)NR is a derivative of the PN2(−) that does not contain the 3′ terminal 46-nt promoter sequence and therefore did not replicate. Please refer to Fig. 3 for sequence details. The number of lesions examined as well as the recombination incidence (defined as the percentage of local lesions on *C. quinoa* leaves that accumulated recombinants) are shown on the right.

Three PN2(−) derivatives [PN3(−), PN4(−), and PN5(−)] were obtained by deleting downstream portions of the PN2(−) antisense region. Portions of PN2(−) that included a short upstream 3′ noncoding sequence and various parts of the antisense region were amplified by PCR using primer 2 in conjunction with primers 4, 5, and 6 for construction of PN3(−), PN4(−), and PN5(−), respectively (Fig. 1). The PCR products were digested with *Spe* I (partially) and *Xba* I and then ligated into PN0 between the *Spe* I and *Xba* I sites.

To generate PN6(−) and PN7(−), the 3′ noncoding region of PN1(−) was amplified by using primer 1 and either primer 7 or 8. The PCR products were digested with *Xho* I and *Eco*RI and ligated between these sites in PN2(−) (Fig. 1). Primer 7 replaced four cytosine residues with four thymine residues. Primer 8 deleted five nucleotides in the upstream part of the PN1(−) antisense region. In addition, it introduced a unique *Bam*HI site several bases downstream of the above deletion (see Fig. 3). PN9(−) was constructed in the same way as PN7(−), but PN2(−) was the template used for PCR. Parts of the 3′ noncoding region of PN7(−) and PN9(−), respectively, were reamplified by PCR using primers 1 and 9, to construct PN8(−) and PN10(−) (Fig. 1). The PCR products were digested with *Bam*HI and *Eco*RI and ligated into PN7(−) that was linearized with the same enzymes. Primer 9 replaced three and four bases with six-base heterologous sequences at two locations in the antisense region of PN7(−) and PN9(−). Sequencing confirmed all the above modifications.

Plant Inoculations. *Chenopodium quinoa*, a local-lesion host, was inoculated with a mixture of 1 μg of each of the following transcribed RNAs: wt RNA1, wt RNA2, and one of the mutated PN*x* RNA3 molecules, as described (6). The accumulation of recombinant RNA was analyzed by Northern blot hybridization (6).

Cloning and Sequencing of Recombinants. Total nucleic acids were extracted from individual lesions and the 3′ end of the progeny RNA3 species was amplified as described (6), by RT–PCR with primers 1 and 2. The resulting cDNA products were digested with an *Eco*RI/*Xba* I mixture and ligated between these sites in the pGEM-3′Zf(−) cloning vector (Promega). Junction sites were determined by sequencing.

RESULTS

Local Complementarity Between BMV RNAs Directs Crossovers. The proposed role of local heteroduplexes in recombination was tested by generating BMV RNA3 molecules that contained a 66-nt insert complementary to wt RNA1 in the upstream part of the mutated 3′ noncoding region (Fig. 1). This RNA3 mutant [designated PN2(−)] was coinoculated with wt RNA1 and wt RNA2 transcripts on leaves of *C. quinoa*, a local-lesion BMV host. Northern blot analysis revealed the accumulation of novel RNA3 molecules that were smaller than PN2(−) RNA3 (Fig. 2*A*). Electrophoresis of RT–PCR-amplified cDNA products revealed size heterogeneity of the 3′ noncoding RNA3 sequences among the recombinants present in separate local lesions (Fig. 2*B*). The five clones examined for each lesion had the same sequences in 90% of the cases (data not shown). This indicated that single types of recombinants predominated in most of the lesions. In 10% of the lesions two types of recombinants were found. Sometimes parental mutant RNA3 molecules coaccumulated with progeny recombinants (as in lanes 13–15 of Fig. 2*B*).

Of 25 RNA3 recombinants isolated from local lesions, all contained RNA1 sequences that crossed within the sequence complementary to the 66-nt antisense PN2(−) region. The acceptor sites were located in or close to the 5′ part of PN2(−) antisense region. Consequently, the RNA3 progeny contained almost the entire 3′ noncoding region taken from RNA1, with the crossovers occurring at nonhomologous positions. Displayed on the putative heteroduplex formed between PN2(−) RNA3 and wt RNA1, the acceptor and donor sites were clustered at or near the left side of the duplex (Fig. 3).

To demonstrate that recombination activity of PN2(−) depended on its antisense region, we tested the *in vivo* stability of two control constructs, PN0 and PN2(+). PN0 RNA3 contains the same 3′ noncoding region as PN2(−) but without the antisense insert, and PN2(+) has the 66-nt RNA1-derived sequence in the sense orientation. Northern blot hybridization as well as RT–PCR analysis (Fig. 2 *A* and *B*, respectively) detected only parental PN0 or PN2(+) RNA3 progeny. Sequencing revealed no recombination or sequence rearrangements among the cloned RT–PCR products.

A selective amplification of the parental RNA3 sequences from a mixture of transcribed mutated RNA3 controls with wt RNA1 and RNA2 allowed us to rule out the possibility that these recombinants were generated by RT–PCR itself. No recombinants were observed (Fig. 2*B*, lanes Φ). Moreover,

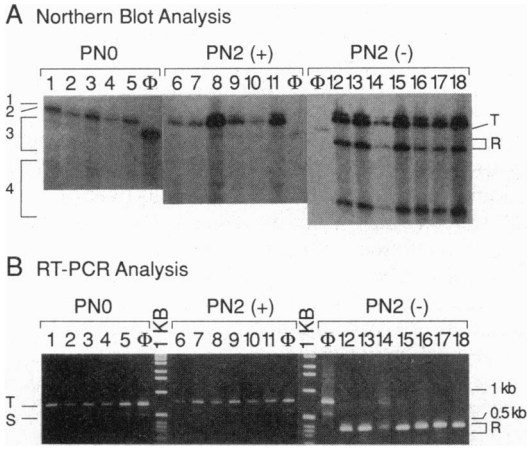

FIG. 2. Characterization of BMV RNA3 recombinants. (*A*) Northern blot analysis of BMV RNA components in total RNAs isolated from local lesions of *C. quinoa*. Progeny RNAs of PN0 (lesions 1–5), PN2(+) (lesions 6–11), and PN2(−) (lesions 12–18) were probed with antisense ^{32}P-labeled RNA transcripts representing the last 200 nt conserved BMV RNA region. Lanes Φ, parental mutant RNA3 transcripts. The position of individual BMV RNA components is shown on the left, and the migration of parental RNA3 transcripts and the progeny recombinants is depicted by the letters T and R, respectively, on the right. (*B*) Electrophoretic analysis of RNA3-specific cDNA obtained by RT–PCR using primers 1 and 2 to amplify the total RNA preparations analyzed in *A*. Control RT–PCR amplifications (lanes Φ) were performed with mixtures of *in vitro* transcribed wt BMV RNA1 and RNA2 and the mutated RNA3 components. The position of PCR products corresponding to the expected length of the parental (inoculated) RNA3 mutants is indicated on the left (T), whereas that for newly emerged recombinants is indicated on the right (R). A standard 1-kb DNA ladder (GIBCO/BRL) is shown in lanes marked 1 KB. Faster-migrating low-intensity bands (S) correspond to artifactual cDNA products that emerged due to weak priming at the boundary of the duplicated 3′ region (see Fig. 1).

the recombinant RNA3 molecules accumulated to high levels within the lesions (Fig. 2*A*).

To confirm the formation of stable heteroduplexes between PN2(−) RNA3 and RNA1, we performed an *in vitro* RNase-protection analysis. RNase-resistant RNA1 fragments of the expected size were obtained after hybridization of nondenatured PN2(−) RNA3 and ^{32}P-labeled wt RNA1 (data not shown). The control reactions with either PN0 or PN2(+) RNA3 did not generate any specific RNase-resistant fragments.

Effects of Modifications in the Antisense Inserts on the Incidence of Recombination and on Crossover Location. To further test the role of antisense inserts in targeting nonhomologous recombination, we determined the effect of the length of the complementary sequence. PN1(−) contained the same 66-bp antisense insert as PN2(−) plus an additional 74-bp inverted RNA1 cDNA sequence (nt 243–382 of RNA1, counted from the 3′ end). Plasmids PN3(−), PN4(−), and PN5(−) contained 40-, 30-, and 20-bp antisense RNA1 cDNA fragments nested at a common RNA1 position, nt 243. Sequencing of cloned, RT–PCR-amplified cDNA products revealed that transcribed PN1(−), PN3(−), and PN4(−), but not PN5(−), generated recombinant RNA3 progeny in *C. quinoa* (Fig. 1). This suggested that an antisense sequence longer than 20 nt is necessary to promote efficient recombination.

The incidence of recombination depended on the length of the antisense sequence (see Fig. 1). The acceptor sites in recombinants obtained with PN1(−) through PN4(−) transcripts clustered within or close to the upstream part of the antisense sequence on RNA3 (Fig. 3). The donor sites clustered within the complementary region of RNA1. All the crossovers were found at or near the left side of the putative heteroduplex (Fig. 3). The lack of recombination in PN5(−) infections indicated, however, that the central and right-side parts of the duplex were also important in recombination, possibly by stabilizing the active left side.

An alternative explanation of the recombination hotspots found in PN1(−) through PN4(−) recombinants is that they might result from selection for viable recombinants. To test the role of selection in recombination, sequence alterations were introduced outside the hotspot sequences observed for PN1(−) through PN4(−) recombinants. The PN6(−) construct allowed for the formation of four weak G·U base pairs at the left side of the putative PN6(−)–RNA1 heteroduplex. Although, compared with the PN1(−) mutant, this did not affect the incidence of recombination (Fig. 1), it shifted the crossover sites toward the central part of the duplex (Fig. 3). This result confirmed the importance of the left-side portion in directing the site of recombination.

The above conclusion was supported by the results obtained with PN7(−) through PN10(−) constructs. Plasmid PN7(−) had a 5-nt deletion in the upstream part of the antisense region as compared to PN1(−). Also, further downstream, it contained a 6-nt heterologous sequence that disrupted the left side of the heteroduplex (Figs. 1 and 3). As in PN6(−), the modification in PN7(−) occurred downstream to recombination hotspot regions of PN1(−)- through PN4(−)-derived recombinants. The acceptor sites in PN7(−)-generated recombinants were shifted downstream on RNA3, while the donor sites were moved upstream on RNA1, compared with those of PN1(−) recombinants. Plasmid PN8(−) contained the same antisense sequence as PN7(−) with two additional downstream mismatch regions (Fig. 1). It generated recombinants with the acceptor and donor hotspots shifted into the central part of the antisense PN8(−) insert and into the RNA1-complementary region, respectively. Compared with PN1(−), the hotspots generated by PN8(−) were 31–84 nt downstream in the RNA3 antisense region and 31–59 nt upstream on RNA1. Consequently, the PN8(−)-generated recombinants had 30–50 and 50–150 more nucleotides in their 3′ noncoding regions than those generated by PN7(−) and PN1(−), respectively. Thus, while the majority of PN1(−)-derived recombinants contained a shorter-than-wt 3′ noncoding region, the PN8(−)-generated recombinants were ≈100 nt longer in this region. In total, the crossovers supported by PN1(−) through PN4(−) were not observed for PN7(−) and PN8(−), although they shared sequences found to be active in PN1(−) through PN4(−). This suggested that the crossovers were primarily determined by the structure of the heteroduplex rather than by selection (see *Discussion*).

Previously, we proposed that partial hybridizations occur between recombining BMV RNAs at the sites of crossovers (5, 6). Constructs PN9(−) and PN10(−) (Fig. 1) were designed to imitate such structures. They could potentially form much energetically weaker heteroduplexes with RNA1 than could PN1(−), PN2(−), PN7(−), or PN8(−). Indeed, PN9(−) and PN10(−) demonstrated a significantly reduced incidence of recombination. The location of recombinant crossovers was within sequences capable of heteroduplex formation (Fig. 3).

To test whether the heteroduplex-driven crossovers could take place between the positive strands, PN2(−)NR, a nonreplicating derivative of PN2(−) RNA3, was examined. PN2(−)NR lacked the last 46 nt of the 3′ RNA replication promoter (25, 26). Consequently, it did not produce a detectable amount of negative strands in barley protoplasts (data not shown). All the lesions generated by PN2(−)NR contained RNA3 recombinants with the crossovers within or in close vicinity to the regions capable of hybridization with

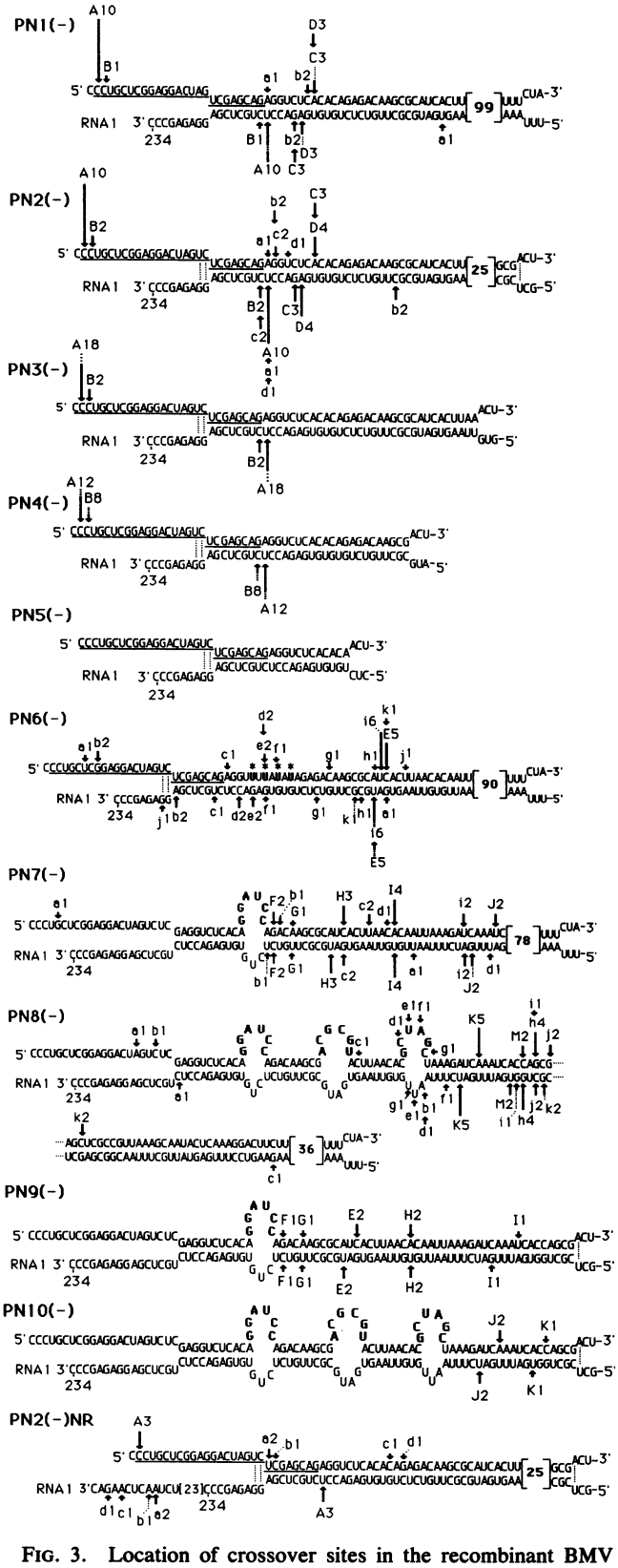

FIG. 3. Location of crossover sites in the recombinant BMV RNA3 molecules generated with PNx constructs. The antisense region of PNx (upper line, in 5′ → 3′ direction) is shown hybridized to the complementary (sense) sequence of the 3′ noncoding region of BMV RNA1 (lower line, in 3′ → 5′ direction). The region of RNA3 that potentially could form a stem-and-loop structure (see below) is underlined. The last nucleotide of the wt RNA1 part and the first nucleotide of a given PNx RNA3 part which are joined in the particular recombinant are depicted by arrows with the same letters on both RNA strands. The size of the arrow is proportional to the number of independent lesions (indicated also by the numbers at the letters) on *C. quinoa* that contained this particular recombinant. Uppercase letters mark those crossover sites that were generated by more than one PNx RNA3 construct, whereas lowercase letters (starting from letter "a" for each heteroduplex) show unique crossover sites. The C → U transitional mutations in PN6(−) are depicted by bold letters with asterisks. The amount of not-shown heteroduplex nucleotides is indicated by numbers in brackets. In addition to the sequences presented, in some lesions some recombinants had nontemplated extra nucleotides at the crossover sites, as follows (numbers in parentheses show the number of lesions that accumulated given recombinants): U in PN6(−)-c (1), PN6(−)-e (1), PN6(−)-E (2), and PN8(−)-e (1); UU in PN2(−)-a (1), PN6(−)-d (1), PN6(−)-e (1), and PN6(−)-E (1); UA in PN2(−)-d (1); UUU in PN6(−)-i (1); UUC in PN1(−)-B (1).

RNA1 (Fig. 3). This suggested that recombination could occur between hybridized positive strands of PN2(−)NR and RNA1 (see *Discussion*).

DISCUSSION

Heteroduplex-Primed Nonhomologous Recombination. The results reported in this communication provide experimental evidence that local complementarity between viral RNA molecules can promote recombination events. The formation of stable double-stranded regions between PNx(−) RNA3 and wt RNA1 molecules was confirmed *in vitro* by RNase protection experiments (data not shown). Constructs that lacked antisense sequences did not generate recombinants and did not form stable duplexes with RNA1 *in vitro*.

The heteroduplex-primed crossover events generated RNA3 recombinants that differed in size from wt and that had almost the entire 3′ noncoding region replaced by that of the RNA1 segment. Because of that and because the crossovers occurred within nonconserved, upstream sequences of the 3′ noncoding region, the recombinants described here can be defined as nonhomologous (illegitimate). Lai (27) differentiates between "regular" and "aberrant" homologous crossovers as those which occur between homologous sequences at symmetrical and asymmetrical locations, respectively. In our system, recombination is driven by sequence complementarity between the recombination substrates rather than by sequence homology. One can envision the involvement of heteroduplexes in homologous or aberrant homologous recombination if double-stranded regions were formed by palindromic sequences.

Effects of Heteroduplex Structure on Recombination Hotspots and Mechanism of Recombination. It has been proposed for coronaviruses that recombination occurs randomly and that the recombination hotspots result from natural selection (26). However, these processes cannot account for the observed differences in the recombination activity of poorly replicating parental BMV PNx molecules. For instance, the fact that PN8(−) did not accumulate the same recombinant classes which PN1(−) and PN7(−) did, although the hotspot sequences of PN1(−) and of PN7(−) were available in PN8(−), strongly supports the importance of hybridized (double-stranded) regions in recombination. Identification of a whole spectrum of RNA3 recombinants which contained 3′ noncoding regions of variable length (between 231 and 403 nt) and a variety of sequences demonstrated that different kinds of crossovers were selectionally permissible. Therefore, the contribution of selection factors for viable recombinants in the observed crossovers must be of limited importance.

The concentration of crossovers in recombinants generated by PN1(−) through PN4(−) was observed at the left side of the heteroduplex (Fig. 3). This can be explained by assuming that the replicase complex did not unwind the double-stranded region efficiently and switched between the

templates before penetrating further downstream. Such a template switching mechanism is supported by the observed shift of the crossovers toward central parts of the heteroduplex when hybridization at the left side was weakened or disrupted. This mechanism is also supported by the presence of nontemplated (mainly uracil residues; see the legend of Fig. 3) nucleotides at the crossover sites. They were probably introduced by replicase stuttering during template switching. Similar results have been shown for recombination in turnip crinkle virus (11, 20).

According to an alternate breakage-and-religation mechanism, preferential cleavage and ligation near the ends of a stable duplex would also explain the concentration of crossovers at the terminal sides. In our system, however, this would be more probable at the right side of the duplex. Digestions at the left side would release the 5′ RNA3 and the 3′ RNA1 fragments, which would be free to dissociate in the absence of complementary sequences. Thus, although not definitely distinguishing between alternate mechanisms of recombination, the observed location of crossovers at the left side is better explained by a template-switching mechanism.

A majority of recombinants had crossovers juxtaposed at or near counterpart nucleotides. Some recombinants, however, had the donor and acceptor crossing sites far apart from each other on or near the heteroduplex. Secondary structure elements were predicted to exist at some crossover sites on the mutated RNA3 molecules (see underlined regions in Fig. 3). This may position the RNA1 and RNA3 sites closer to each other, thus allowing the viral replicase to switch templates at more-upstream RNA3 locations.

In the heteroduplex-mediated system, recombination could occur between either two negative or two positive strands, which could lead to similar recombinants. The recombination competence of a nonreplicating construct, PN2(−)NR, as well as other previously reported BMV RNA mutants (8, 9) strongly suggests that the recombination events can occur between positive strands during negative-strand synthesis. Also, hybridizations between positive strands are more likely than hybridizations between negative strands, simply because positive-stranded RNA is much more abundant than negative-stranded RNA in BMV infections (28).

In addition to providing the experimental evidence for the heteroduplex-primed model (5, 6), the targeting system described here offers unique opportunities for studying the mechanism of nonhomologous recombination among RNA viruses. The recombination activity of various BMV replicase mutants needs to be tested in order to examine the involvement of viral replicase proteins during recombination. Theoretically, the heteroduplex-mediated recombination could be widely used for targeting recombinant crosses into different RNA regions. It remains to be demonstrated whether the heteroduplex-driven mechanism could operate in other regions on the BMV genome or in other RNA viruses.

We thank M. Altschuler, S. Flasinski, A. Gordon-Walker, S. Guy, M. Hudspeth, R. Meganathan, S. Schlesinger, J. Stafstrom, and B. G. Weiss for comments and discussions. This work was supported by a grant from the National Institute for Allergy and Infectious Diseases (RO1 AI26769) and by the Plant Molecular Biology Center at Northern Illinois University.

1. Strauss, J. H. & Strauss, E. G. (1988) *Annu. Rev. Microbiol.* **42,** 657–683.
2. King, A. M. Q. (1988) in *RNA Genetics*, eds. Domingo, E., Holland, J. J. & Ahlquist, P. (CRC Press, Boca Raton, FL), Vol. 2, pp. 149–165.
3. Ahlquist, P., Dasgupta, R. & Kaesberg, P. (1981) *Cell* **23,** 183–189.
4. Bujarski, J. J. & Kaesberg, P. (1986) *Nature (London)* **321,** 528–531.
5. Bujarski, J. J. & Dzianott, A. M. (1991) *J. Virol.* **65,** 4153–4159.
6. Nagy, P. D. & Bujarski, J. J. (1992) *J. Virol.* **66,** 6824–6828.
7. Rao, A. L. N., Sullivan, B. P. & Hall, T. C. (1990) *J. Gen. Virol.* **71,** 1403–1407.
8. Rao, A. L. N. & Hall, T. C. (1990) *J. Virol.* **64,** 2437–2441.
9. Ishikawa, M., Kroner, P., Ahlquist, P. & Meshi, T. (1991) *J. Virol.* **65,** 3451–3459.
10. Allison, R., Thompson, C. & Ahlquist, P. (1990) *Proc. Natl. Acad. Sci. USA* **87,** 1820–1824.
11. Cascone, P. J., Carpenter, C. D., Li, X. H. & Simon, A. E. (1990) *EMBO J.* **9,** 1709–1715.
12. Van der Kuyl, A. C., Neeleman, L. & Bol, J. F. (1991) *Virology* **183,** 731–738.
13. Kirkegaard, K. & Baltimore, D. (1986) *Cell* **47,** 433–443.
14. Romanova, L. I., Blinov, V. M., Tolskaya, E. A., Victorova, E. G., Kolesnikova, M. S., Guseva, E. A. & Agol, V. I. (1986) *Virology* **155,** 202–213.
15. Kuge, S., Saito, I. & Nomoto, A. (1986) *J. Mol. Biol.* **192,** 473–487.
16. Makino, S., Keck, J. G., Stohlman, S. A. & Lai, M. M. C. (1986) *J. Virol.* **57,** 729–737.
17. Weiss, B. G. & Schlesinger, S. (1991) *J. Virol.* **65,** 4017–4025.
18. Munishkin, A. V., Voronin, L. A. & Chetverin, A. B. (1988) *Nature (London)* **333,** 473–475.
19. Palasingam, K. & Shaklee, P. N. (1992) *J. Virol.* **66,** 2435–2442.
20. Zhang, C., Cascone, P. J. & Simon, A. E. (1991) *Virology* **184,** 791–794.
21. Banner, L. R. & Lai, M. M. C. (1991) *Virology* **185,** 441–445.
22. Janda, M., French, R. & Ahlquist, P. (1987) *Virology* **158,** 259–262.
23. Allison, R. F., Janda, M. & Ahlquist, P. (1988) *J. Virol.* **62,** 3581–3588.
24. Sambrook, J., Fritsch, E. F. & Maniatis, T. (1989) *Molecular Cloning: A Laboratory Manual* (Cold Spring Harbor Lab. Press, Plainview, NY), p. 7.71.
25. Miller, W. A., Bujarski, J. J., Dreher, T. W. & Hall, T. C. (1985) *J. Mol. Biol.* **187,** 537–546.
26. Bujarski, J. J., Ahlquist, P., Hall, T. C., Dreher, T. W. & Kaesberg, P. (1986) *EMBO J.* **5,** 1769–1774.
27. Lai, M. M. C. (1992) *Microbiol. Rev.* **56,** 61–79.
28. Marsh, L. E., Huntley, C. C., Pogue, G. P., Connel, J. P. & Hall, T. C. (1991) *Virology* **182,** 76–83.